

Signal Canceller in the Carrier Super-positioning Satellite Networks

Mayumi Osato

Graduate School of Information Science, Nara Institute of Science and Technology (NAIST), Nara, Japan
Email: mayumi-o@is.naist.jp

Hiroyuki Kobashi, Robert Y. Omaki, Takao Hara and Minoru Okada

Graduate School of Information Science, Nara Institute of Science and Technology (NAIST), Nara, Japan
Email: hiro-kob@is.naist.jp, omaki@synthesis.co.jp, {takao-ha, mokada}@is.naist.jp

Abstract—To establish the interference canceller, generating replicas of unwanted carriers is a key. This paper addresses the design and performances of two types of signal canceller that are used for two typical types of satellite communications, namely P-MP VSAT (Point-to-Multi-Point Very Small-Aperture Terminal) and P-P (Point-to-Point) paired carrier systems. For P-MP VSAT, we show a simplified method where a replica of an unwanted carrier is generated by demodulating it. We have developed a reference simulator to simulate the behavior and performance. This simulator takes into account degradation due to implementation. The source code developed here is applicable to the implementation of FPGA. We also propose a method to generate replicas by stably measuring the satellite round-trip delay by multi-component code (MCC) on a real-time basis for P-P, since we cannot apply the same method to this case as we can for VSAT systems. We use MCC (Multi-component Code) to measure the delay as quickly and accurately as possible. It is the key how stably the acquisition of the code is established in the actual environment of satellite channel which is suffered from heavy noise and large level variation. We show a method to stabilize acquisition process of MCC by normalizing multi-level correlation using a level obtained by additional loop.

Index Terms— satellite communications, frequency re-use, interference canceller, multi-component code, acquisition and synchronization

I. INTRODUCTION

Carrier super-positioning is a promising method capable of assigning inbound and outbound signals in the same frequency band. It is for the efficient use of frequency in the satellite communications as well as the improvement of information security. Over the last few years, several studies have reported on schemes for generating replicas for signal cancellation [1],[2]. A typical method of generating replicas is to demodulate unwanted signals from received ones [3]. Another method is to measure the satellite round-trip delay to synchronize the timing of replicas with the received signals [4] [5] or by using real-time information on the satellite's orbital position in space [6]. Among these methods, the first one [3] is applicable only for a network

in which the level of unwanted signals is higher than that of wanted ones such as in a P-MP VSAT network.

For a P-MP system, we report in this paper the performance and behavior of the signal canceller, which we verified by computer simulations using a digital signal processing technique. The simulator developed here takes into account the effect of implementation loss, such as A/D converter quantization error and calculation error, due to finite length numeric value expressions.

In the former method, where a replica is generated by demodulation, there are three key points in creating an accurate canceller. One is to design the transmission path characteristics. The second is to adjust the timing of both signals, and the third is to put AGC (Automatic Gain Control) before the canceller.

The proposed canceller for a P-MP system cannot be applied for P-P systems, because the strengths of wanted and unwanted signals are at the same level. That is, the unwanted signals cannot be demodulated. To solve this problem, replica of each unwanted signal must be generated from the transmitted signal. The canceller measures the satellite's delay and generates replicas by making the same delay for the transmitted signals. In this scheme, the key is to achieve an accurate and stable delay measurement. In Section 4, we propose a measurement method for one-round-trip delay, a delay tracking loop that is stable at very low C/N conditions.

Multi-Component Code (MCC) is proposed for delay tracking. The MCC has very superior performance on the acquisition time comparing to the conventional method which uses single code. The acquisition and synchronization of MCC can be achieved by using the property of different but determined multi-value auto-correlation. In practice, however, because of this multi-level correlation property, it is more affected by the noise and the receiver input level, resulting in a decision error of correlation. The delay tracking loop shall thus be designed to behave stably against such heavy noise and input-level variation. A method to stabilize the correlation detector is proposed here by which multi-level correlation value is normalized by a value which can be obtained by an additional loop. And the effectiveness of

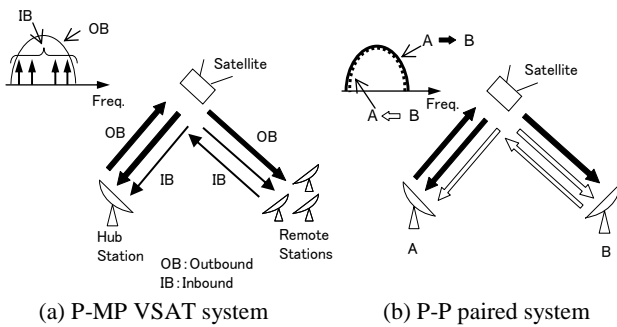


Figure 1. Carrier allocation for carrier super-positioning of P-MP and P-P

this method is verified by simulating the acquisition process and time for various cases of input level change.

II. SYSTEM DESCRIPTION

Figure 1 shows the carrier super-positioning of two typical satellite communications networks. Figure 1(a) shows a P-MP system in which both out- and inbound carriers are allocated to the same band, though they are separated in a conventional system. The outbound (OB) carrier has a higher power density than that of inbound (IB) carriers because of the difference in G/T between Hub and remote stations. All remote stations can receive the OB as it is since OB is much stronger than IB. However, as shown in Fig. 1(a), the OB carrier that is sent from the Hub station has to be cancelled at the Hub because the Hub wants to receive IB, the level of which is lower than OB. Figure 1(b) shows the case of a P-P system where both carriers are sent at an equal level in the same band. The network is composed of high speed paired carriers. In this system, we need to cancel the unwanted carrier at both stations.

III. CANCELLER FOR P-MP VSAT SYSTEM

A. Configuration of signal canceller

Figure 2 shows a basic block diagram of a canceller. This canceller is put in the Hub station in front of demodulators of IB carriers. The received signal is divided into two paths. In Path 2, the unwanted OB is demodulated from the outbound signal (OB is the carrier sent by the Hub) and modulated again. On the other hand, the received signal passes through Path 1 where no processing is done other than that the signal is delayed by the time duration that Path 2 needs to demodulate (τ in Fig. 2). The replica, which is synchronized with the received signal, is subtracted from the received signal. However, some power remains if there exists any difference between those that cause interference to IB carriers.

To make the replicas as precise as possible, we first designed the filter characteristics of Path 2 so as to adjust the filter characteristics of both paths, after which the delay between the two paths is adjusted. The canceller output is fed back to the gain control of the replica's amplifier. In this case, the AGC control voltage shall not be affected by the power of wanted IB carriers. Therefore,

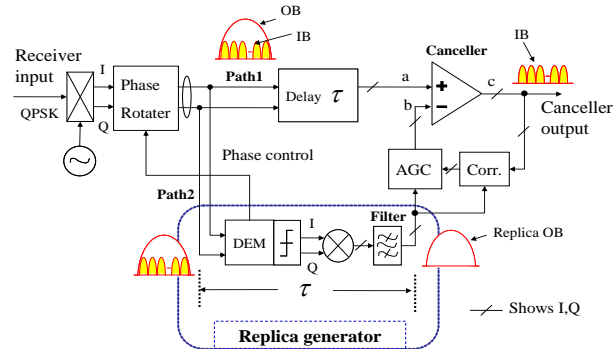


Figure 2. Block diagram of signal canceller for P-MP VSAT system

TABLE I. SPECIFICATIONS OF DIGITAL PROCESSING P-MP CANCELLER

Items	Specification
Data rate of OB carrier (QPSK)	5, 10, 20 Msymbol/s
Data rate of IB carriers (QPSK)	64 k, 1 M, 3 Msymbol/s
D/A conversion	12 bit/sample
Sampling rate	72 MHz
Receive filter	Root raised cosine($\alpha = 0.35$)
Difference of power density between OB and IB carriers	10 ~ 13 dB
Carrier & timing tracking	yes
Input level variation	2 dB
Cancellation of unwanted OB	>30 dB

we adopted the processing scheme in the AGC by which we calculate the correlation between canceller output and the replica so that we can acquire the control voltage which is derived only by the power difference between the unwanted carrier and the replica.

The system specifications of the simulator are shown in Table I.

B. Simulated Performance

The simulator is written in C++ and takes into account the degradation due to quantization errors, calculation errors and so on. As mentioned above, the level of wanted carriers (IB) for the Hub station is lower than that of unwanted (OB) carriers. Let us assume the difference is 13 dB, the compression of unwanted carriers shall be more than 26 dB in order to get a C/I of wanted carriers (IB) of more than 13 dB.

Figure 3 shows the result of the computer simulation for cancellation of unwanted OB at the canceller's output. Spectra of OB both before and after cancellation are shown here. Figure 4 shows the wave forms for channel I of OB and its replica just at the input of the canceller (points "a" and "b" in Fig. 2) and the remaining signal at the canceller's output (point "c" in Fig. 2). Figure 5 shows the spectrum in the case where we put one wanted carrier (IB) of 1 Msps QPSK. The larger one is the spectrum of a mixture of a 5-Msps OB and one 1-Msps IB, and the smaller one is extracted wanted IB for which the power density is 13 dB lower than OB. It is shown that the wanted IB is extracted from the mixture of both IB and OB.

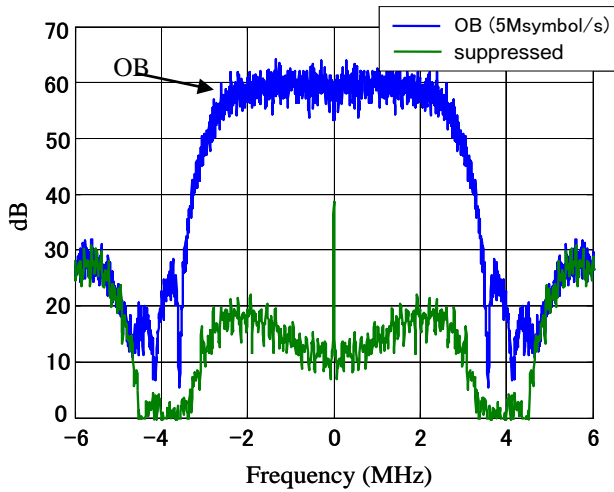


Figure 3. Spectrum of OB carrier of canceller input and output (Noise free)

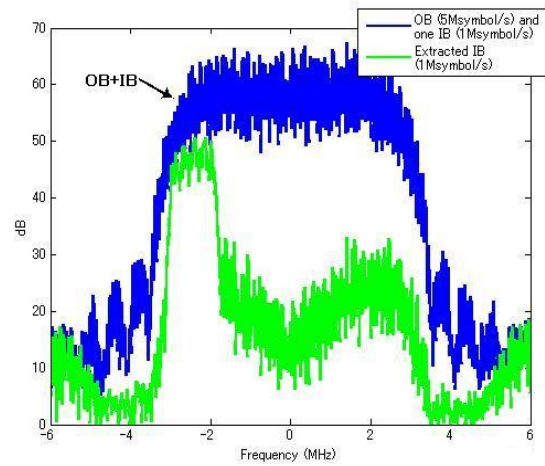


Figure 5. OB and extracted IB (Noise free, Level difference 13dB)

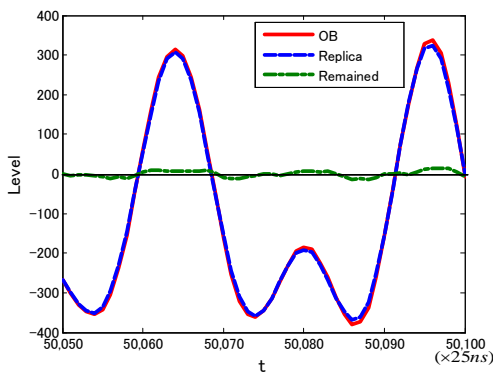


Figure 4. OB signal and generated replica and remained signal

Thus, Fig. 6 shows the performance of AGC. Once the level of the input signal deviates, the difference appears directly in the canceller output as interference if the canceller has no AGC function. This is because the level at the canceller output changes while the replica level stays nominal if the receiver input changes. It is verified that the AGC performs well against the input-level variation of ± 1 dB, which is specific to this system. (It is assumed that another AGC is provided in the satellite receiver to the compress the level of change up to about ± 1 dB.)

IV. CANCELLER BY DELAY MEASUREMENT FOR P-P

A. Required accuracy of replicas

As mentioned above, a replica cannot be generated by demodulating unwanted signals in a P-P, since both wanted and unwanted carriers are superposed in the same band at an equal level. Figure 7 shows a block diagram of the proposed canceller for P-P. Data replicas can be obtained by shifting one's own data once the round-trip delay has been precisely measured. To generate a replica, we need the data and carrier to be precisely synchronized with the received signal.

In this study, we concentrate on how to measure the data timing as accurately and stably as possible. In the previous study [4], we found that extremely accurate

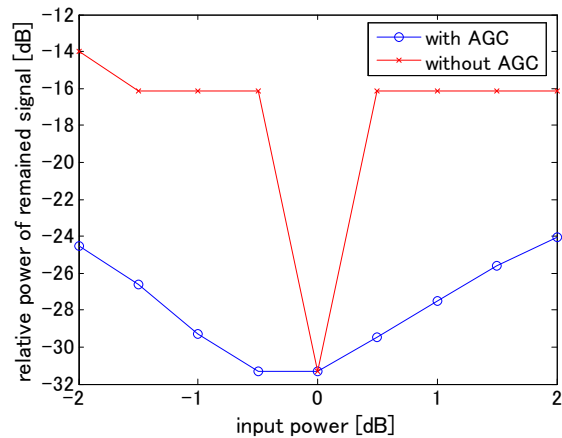


Figure 6. AGC performance

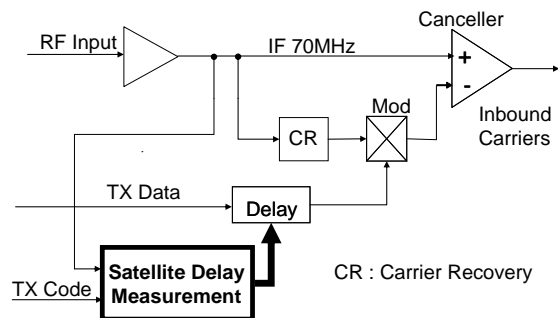


Figure 7. Block diagram of canceller

measurements must be made of the delay time for one round trip in increments of 3° to 5° (about 1/100 symbol). We often use code for delay measurement. The conventional method employing a single code includes the problem that the acquisition time becomes too long. It is estimated that the code level shall be -25dB or less than main signals so that S/N degradation given to main signal is less than 0.1 dB assuming that it is operated at $S/N=10$ dB. Thus the code synchronization loop has to operate under very low C/N . Consequently, in this study, using MCC for delay measurement, we propose a design

				$W = X \oplus (Y \cdot Z)$					$w = x \oplus (y \cdot z)$					
				z	0	1	0	1	0	1	0	1	0	1
				y	0	0	1	1	0	0	1	1	0	1
				x	0	0	0	0	1	1	1	1	1	
Z	Y	X	W/w	0	0	0	1	1	1	1	1	0		
0	0	0	0	0	0	0	1	1	1	1	1	0		
1	0	0	0	0	0	0	1	1	1	1	1	0		
0	1	0	0	0	0	0	1	1	1	1	1	0		
1	1	0	1	1	1	1	0	0	0	0	0	1		
0	0	1	1	1	1	1	0	0	0	0	0	1		
1	0	1	1	1	1	1	0	0	0	0	0	1		
0	1	1	1	1	1	1	0	0	0	0	0	1		
1	1	1	0	0	0	1	1	1	1	1	1	0		

(agreement ; 0, disagreement ; 1)

Figure 8. Auto-correlation matrix for MCC $W = X \oplus (Y \times Z)$

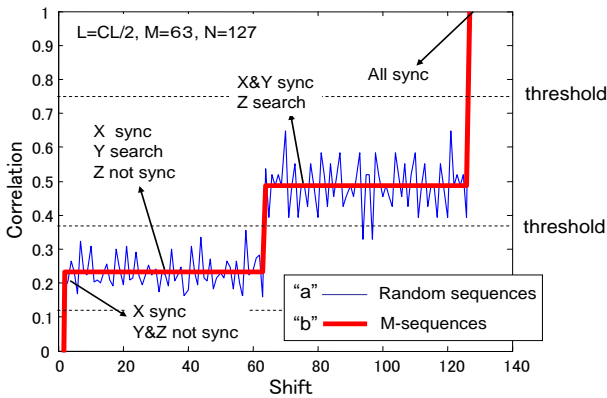


Figure 9. Acquisition process of MCC

method to measure the delay stably and show the acquisition performance of proposed method in the conditions which has heavy noise and large level variation.

B. Design of MCC at low C/N

We often use matrices to find the correlation property of MCC [7]. Figure 8 shows the correlation matrix of MCC $W = X \oplus (Y \times Z)$ in which X, Y, and Z are the component codes, \oplus is exclusive-or, and \times is a multiplication. By using the MCC, the acquisition time is reduced on average to $(L+M+N)/LMN$ times of conventional single code, where L, M, and N are respectively the length of each component code if there is no common factor among them. Considering the auto-correlation of W by this matrix, the correlation C is 0 when all components are out of phase, 0.25 when code X is in phase, 0.5 when X and Y are in phase and 1.0 when all are in phase [7].

Figure 9 shows the transition of the correlation for acquiring this code. In our MCC, a clock with a length of 2 is used for code X. We also consider two cases where both random and M-sequences are used for codes Y and Z.

The distance to the geostationary satellite is about 36,000 km and the delay time is about 250 ms. The satellite's orbit drifts by about 0.66 (0.33x2) ms.

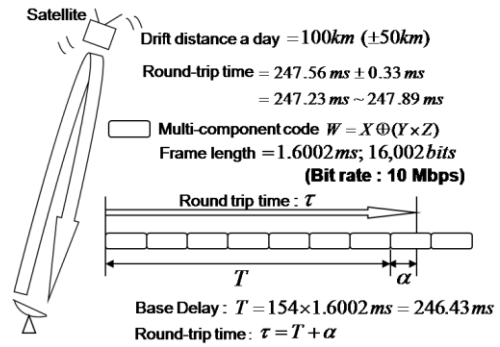


Figure 10. Configuration of MCC

We propose here to use the MCC, which includes the half-clock rate ($CL/2$) as code X, and 63 and 127 code lengths for Y and Z, respectively. As shown in Fig. 10, the length of this code is 16,002 bits, and the delay is 1.6002 ms when the rate is 10 Mbps. One round-trip includes $154 + \alpha$ ($\alpha < 1$) frames. Thus, the issue here is to measure and track only α because 154 are always common. The codes are transmitted 25 dB lower than the main carrier.

C. Acquisition and synchronization

We use the MCC, which includes sequences whose lengths are 2, 63, and 127. Time for acquisition is the sum of the time for searching three component codes.

Figure 11 depicts the decision-error model. In noisy conditions, a decision error may occur for multi-level correlation values, T1, T2, and T3 in Fig. 11 are the thresholds. Table II shows the phase search algorithm of this code. When the S/N is specified, the noise distribution at each correlation level remains the same. The thresholds are set in the middle of the correlation. In Fig. 11, p1 is the probability that an upward or downward

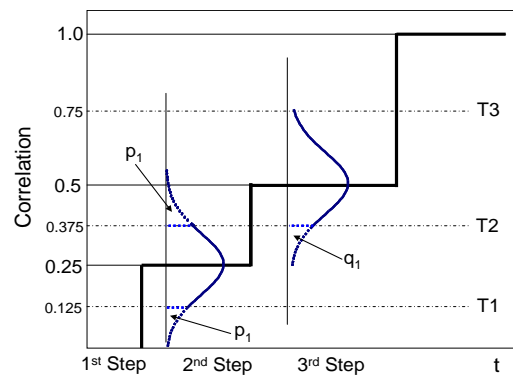


Figure 11. Configuration of MCC

TABLE II. PHASE SEARCH LOGIC FOR EACH COMPONENT CODE

1 st step	2 nd step	3 rd step	4 th step
Clock($CL/2$) synch by COR2 loop	$C < 0.375$ Y search	$0.375 \leq C < 0.75$ Z search	$0.75 \leq C$ Acq. completed

(C:Correlation value)

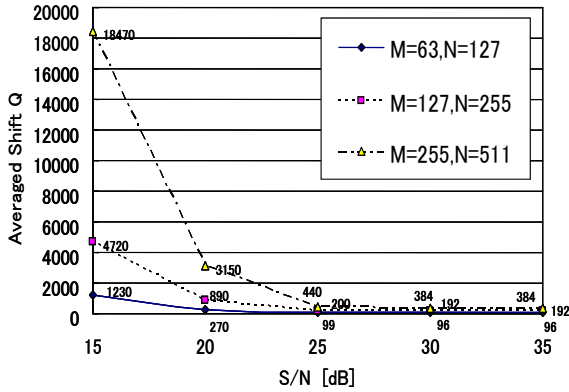


Figure 12. Average number of shifts

error to a neighboring step occurs in the second step, and q_1 is the probability that an error occurs in the third step to the second one. If such an error occurs, acquisition time is delayed.

Figure 12 shows the averaged steps for acquiring the particular code used here as a function of the S/N at the output of the correlator. The results in this figure refer to the theoretical equation [8].

S/N is improved by lengthening the integration time. Table III shows the relationship between integration time and average time of acquisition. The results in the table suggest that it would be reasonable to choose the integration of 10^5 bits, and that acquisition takes about 1 sec on average.

TABLE III. ACQUISITION TIME

Integration for correlation [bit]	10^6	10^5	10^4
S/N Improvement [dB]	60	50	40
S/N_{out} [dB]	+35	+25	+15
Average Shift Q	96	99	1280
sec/shift [s]	0.1	0.01	0.001
Average Acquisition time [s]	9.6	0.99	1.28

(Bit rate: 10 Mbps, S/N_{IN} : -25 dB)

D. Code selection for MCC

Acquisition of this code is achieved by detecting the four level correlations. Figure 8 shows that these correlations are true under the assumption that each component code is long enough and statistically random. However, the codes may not necessarily be so long. It is important, therefore, to know whether the correlation still takes four nominal values for such short lengths of code regardless of the phase shift of each component code. We calculated the correlation value. In Fig. 9, “a” denotes the transition of the correlation when random sequences are used as component codes Y and Z , while “b” indicates what happens when M-sequences are used. A noticeable difference can be observed between these two cases: transition “a” deviates a long way from its nominal for the phase shift of each component code. If the correlation deviates from the nominal value, the error probability of the status decision increases. Furthermore, “a” sometimes exceeds the threshold without noise. This

result indicates that it is difficult to use random sequences as component code. On the other hand, “b” is very stable. We found the auto-correlation of this code takes constant value in step 2 and 3 when M-sequences are used for Y and Z .

E. Stable acquisition of the loop

The threshold for detecting the correlation level becomes marginal and unstable when the input signal level varies. We propose here a loop design that offers consistently stable operation. Figure 13 depicts a block diagram of the system. This system features two loops and three correlators. The loop including correlator 2 (COR2) is for clock acquisition and COR1 is for codes Y and Z . COR2 is the correlator between input signal W and the half-bit-shifted clock ($CL/2$). The correlation between W and $CL/2$ is easily obtained using the matrix in Fig. 14, being 0.5 when both received and local clocks are in phase and -0.5 when there is an inverse phase. In accordance with this property, the correlation at points

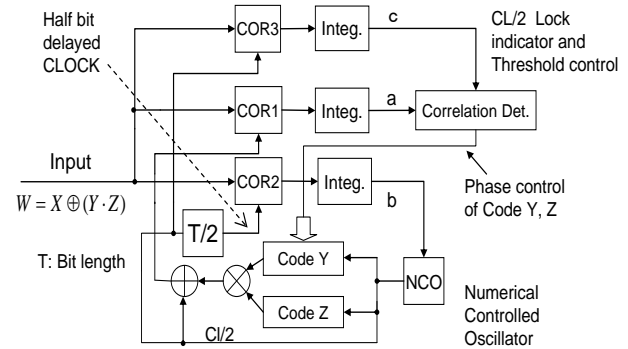


Figure 13. Block diagram of MCC

Z	Y	CL/2	W	0	1
0	0	0	0	0	1
1	0	0	0	0	1
0	1	0	0	0	1
1	1	0	1	1	0
0	0	1	1	1	0
1	0	1	1	1	0
0	1	1	1	1	0
1	1	1	0	0	1

(agreement ; 0, disagreement ; 1)

$$C_{inphase} = \frac{6-2}{8} = 0.5$$

$$C_{inverse} = \frac{2-6}{8} = -0.5$$

Figure 14. Cross-correlation matrix between $W = CL/2 \oplus (Y \times Z)$ and clock $CL/2$

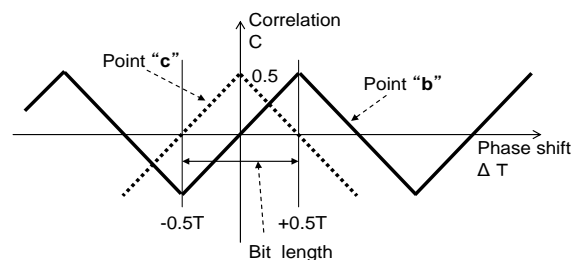


Figure 15. Correlation at points “b” and “c” in Fig. 13

“b” and “c” is shown in Fig. 15 as a function of clock phase error. It has been confirmed by the computer simulation. The correlation at point “c” is always constant at 0.5 as long as the clock is synchronized. Once the clock is acquired, the correlation at point "a" becomes 0.25 (second step in Fig. 11). This value may be varied if the input level is changed. However, after the integration of correlator 3 (COR3) with enough time for smoothing, the threshold for detecting steps 3 and 4 can be calibrated by normalizing “a” by “c” which is obtained at the output of COR3. For example, if the correlation at COR3 is 30% higher than a nominal value (namely, 0.5×1.3), the threshold of two other steps shall be set 30% higher than the nominal. This method makes it possible to stabilize acquisition.

F. Acquisition process by computer simulation

The performance and characteristics of acquisition of the MCC conducted by simulation are shown here by changing C/N. The acquisition performance against to the input level variation has also been simulated in order to verify the effect of stabilization of correlation level mentioned in 4-E. Table IV shows the major parameter of this simulation. The major issue of the performance is the acquisition time. In order to get mean time to complete acquisition, we assumed that the acquisition starts from just half way of phase difference of each component code though it is normally necessary to simulate all cases of initial phase difference between receiving component

TABLE IV.
SIMULATION PARAMETERS OF MCC

Items	Specifications
	$W = X \oplus (Y \times Z)$ (code length 16,002)
Multi-component code	(\oplus is exclusive or, \times is multiply) X ; CL/2 (code length 2) Y ; M-sequence (code length 63) Z ; M-sequence (code length 127) X ; 1, Y ; 32, Z ; 64
Initial phase error	(a half for each component code)
Number of acquisition trials for each C/N	100

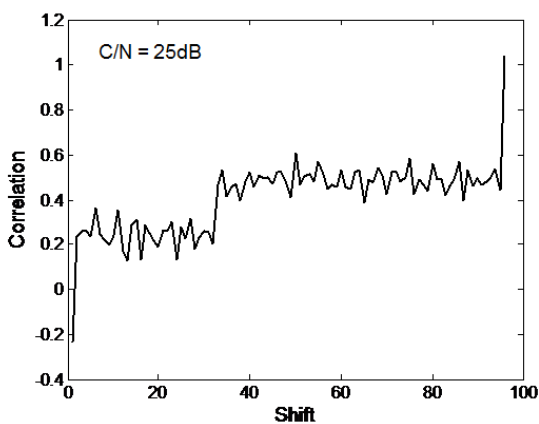
codes and locally generated codes. for each component code. This is to save the time required for simulation. The simulation has been conducted by adding Gaussian noise derived from computer.

1) Acquisition process

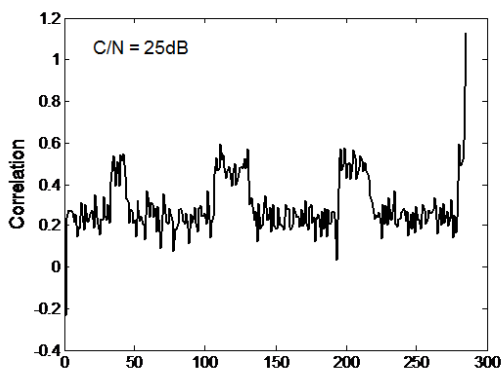
Two example of acquisition process are shown here in Fig.16 for the MCC of which component code length are $CL/2=2, Y=63$ and $Z=127$. Figure 16 (a) is the case where no errors occurred until acquisition is completed and Fig.16(b) shows the case it is completed after several errors occurred. The former acquires the MCC within a period of the sum of initial phase error of code Y and Z ($96=32+64$) though the latter takes about 280 times of phase shift. Figure 17 shows the distribution of acquisition time over the trials of 100 acquisitions which start from the same initial phase errors, that is from half way. As shown in Fig. 17, in some cases it takes more than 500 phase shift. In this simulation, the completion of the acquisition is determined by the criterion that the correlation value reaches to more than 0.75 and that all component codes are in phase. However in actual case, the correlation level is an only criterion. Therefore, it is very important to avoid false detection by adopting “double check” at the last step of acquisition. This is called here as “forward protection”. The effects of forward protection are described later.

2) The effects of input level change against to the acquisition performances

When receiving level of the code varies by some



(a) The case no error occurs



(b) The case some error occurs

Figure 16. Two example of a acquisition process of multi-component code

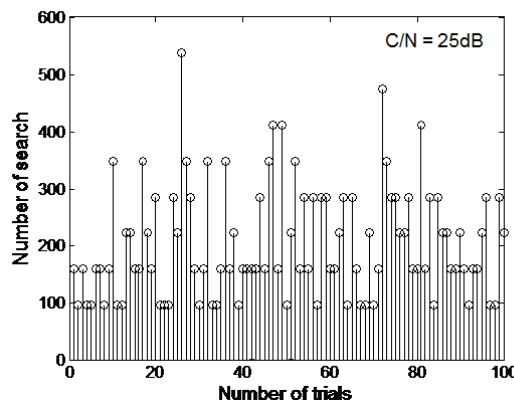


Figure 17. A distribution of number of phase search in 100 trials (C/N=25dB)

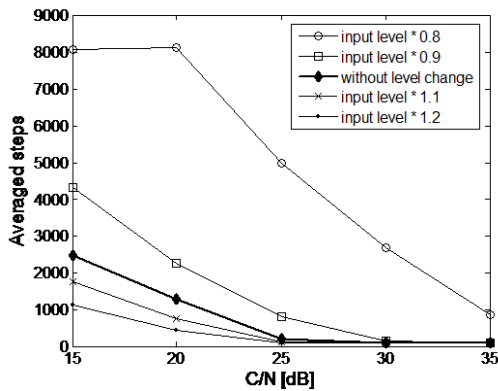


Figure 18. Average acquisition time as a function of C/N for various input level

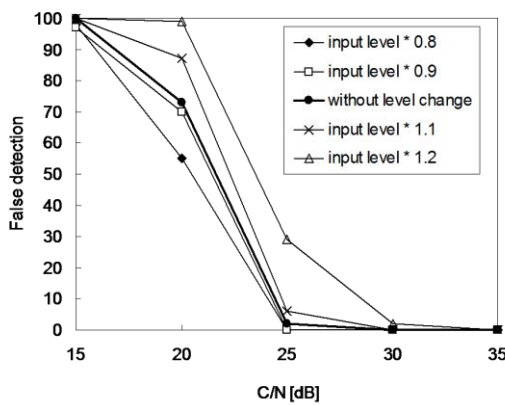


Figure 19. False detection probability for various input level

reasons at the input of MCC tracking loop, the correlation level shown in Fig.11 proportionally varies too and the acquisition performance would be fatally degraded if stabilization is not adopted. It is common to put AGC (Automatic Gain Control) at IF or RF of satellite receiver. However, the AGC does not precisely control the low level MCC code but controls total power of received signal. Thus the code level can be varied by the attenuation like very rapid rain fall or by the change of number of access carriers.

a) *Acquisition time:* Figure 18 shows the averaged acquisition time of the same code as a function of integrator output C/N , $(C/N)_{out}$ for various input level assuming that proposed method of stabilization is not adopted. The phenomena which we can predict for the level variation are as follows. (1) the detection error towards lower level will increase when input level decreases, (2) the error towards higher level will increase when input level increases. If the error probability towards lower level increases, the loop shifts the code phase which has already been acquired and causing the penalty of reacquisition of maximum length of the code. In Fig. 17, the delay size of 63 which often appears comes from that the 3rd step is mis-detected to 2nd step.

Then, let's see the case when the input level increases in Fig.18. A mysterious phenomenon which shortens the time when input level increases can be observed. This is

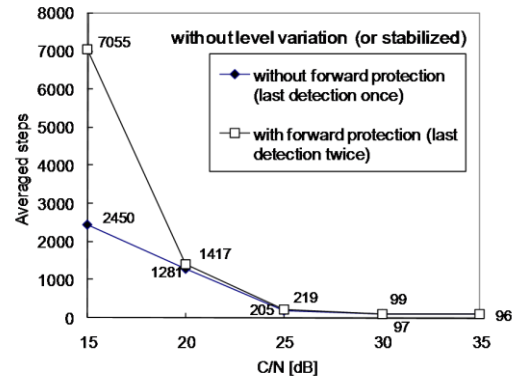


Figure 20. Average acquisition time for two cases of the last detection

because that the error probability to backward decreases and decreases the penalty of reacquisition for code already acquired. The bold line in Fig. 18 shows the case input level is kept nominal. This line is also the case that the input level is stabilized by our method however the input level varies.

b) *False detection:* The false detection is determined in the simulation by the case that the correlation reached to the level larger than 0.75 but the phases are still not in-phase. The probability of false detection is shown in Fig. 19 for 100 acquisition trials. It rapidly increases when the C/N is getting less than 25dB. The probability also increases as the input level raises. The bold line in Fig.19 is the case that the input level is kept nominal or can be considered as the case the stabilizing method is adopted for four other cases.

G. Performance improvement by search method

1) Forward protection

In order to reduce the probability of false detection at the last step (3rd to 4th step), the criteria by which acquisition completion is judged when the correlation exceeds 0.75 in two consecutive decisions is adopted. Figure 20 shows the effects of forward protection on the averaged acquisition time. The averaged time for the case forward protection is adopted is longer than the case it is not adopted at the region C/N is below 20dB. This is because that the phase of code Z is wrongly shifted if the correlation is below 0.75 by miss-detection at the second judgment.

Then, the false detection is evaluated in Fig.21. Figure 21 shows that the probability is drastically reduced by forward protection. Bold line is the case input level is kept nominal and can be considered as the case proposed stabilizing method is adopted.

2) Backward protection

Here we discuss the backward protection. Backward protection means the double check of varies of the correlation level from upper step to lower step. The loop does not shift the phase of lower step code unless the detected correlation is below the threshold consecutively two times. By this protection, wrong shift of code which is already in phase is protected.

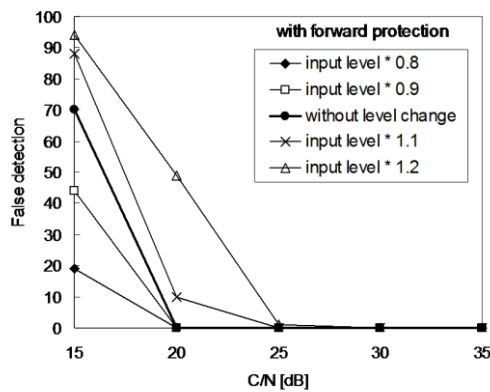


Figure 21. False detection probability for various input levels

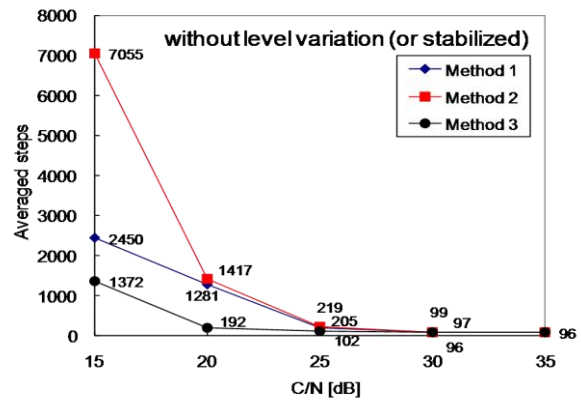


Figure 22. Average acquisition time for three methods

H. Improved over all performance

The averaged acquisition time and the false detection probability for the method both forward and backward protections are adopted (method 3) in Figures 22 and 23 respectively on a comparison with two other methods of non protection (method 1), and forward protection only (method 2). Table V shows the comparison of these three methods. It is clear that method 3 has superior performance for acquisition time and false detection among these three methods.

Generally false detection gives fatal damage on the system. The required performance for false detection probability depends on the system. In many cases, false detection cannot be allowed. However in the case of carrier super-positioning, the retry may be allowed in such case that canceller does not work by the operation of the network.

In any case as shown in Fig. 23, the false detection probability can be almost zero in the region C/N is larger than 25dB.

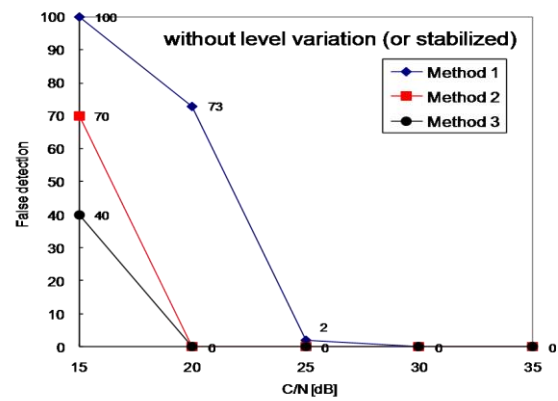


Figure 23. False detection probability for three methods

TABLE V.
COMPARISON OF THREE METHODS

Method	1	2	3
Description	No protection	Forward protection at the last stage	Forward protection at the last stage + Backward protection at 3 rd to 2 nd stage
Acquisition time	△	×	○
False detection	×	○	○
Over all	×	△	○

V. CONCLUSION

We showed solutions for frequency reuse of satellite communications by proposing two types of signal canceller. One is a simplified method to generate replicas by demodulating unwanted carriers for P-MP systems.

Simulation results show that this method is feasible for P-MP VSAT networks.

The other is the method to generate timing of replica by measuring satellite delay by a delay tracking loop that behaves stably in the level-changeable conditions for P-P. Here we proposed using multi-component codes to measure delay. And we showed the design and length of codes, as well as important loop constants for acquisition such as the integration period for correlation by conducting computer simulation of the loop in the environment of heavy noise and level change, in order that the system provides accurate fast and stable synchronization.

In the case of satellite communications, the frequency of up-link and down-link are different, so we can cancel the unwanted signal relatively easy compared with other communications such as wire line.

ACKNOWLEDGMENT

Authors would like to thank JSAT corporation for their support of this research.

REFERENCES

[1] Noriaki ISHIDA, "Common-band Satellite Communication System", IEIEC Transactions Vol. J82-B, No.8, pp1531-1537, Aug. 1999.

- [2] Hideki Toshinaga, Kiyoshi Kobayashi, Kohei Ohata and Hiroshi Kazama "Interference Cancellation for Multimedia Satellite Communication Systems Employing Superposed Transmission", Technical Report of IEICE, SAT2000-86, Dec. 2000.
- [3] M. Osato, H. Kobashi, T. Hara, M. Okada and H. Yamamoto, "Simplified Cancellor for Multi-level Modulation Super-positioning for Frequency Reuse Satellite Communications," ICT2006, May, 2006.
- [4] M. Ichikawa, T. Hara, M. Okada, H. Yamamoto and K. Andou, "Fast and Accurate Cancellor on Carrier Super-positioning for VSAT Frequency Reuse," IEEE-WCNC 2005, New Orleans, March, 2005.
- [5] H. Kobashi, M. Osato, T. Hara, M. Okada and H. Yamamoto, "Signal Cancellation for Satellite Frequency Reuse by Super-positioning multi-level Modulation," IEEE-ISCC2006, June, 2006.
- [6] N. Ishida, "Common-band Satellite Communication System," IEICE Transactions Vol. J82-B, No.8, pp1531-1537, Aug. 1999.
- [7] S.W. Golomb and M.F. Easterling, "Digital Communications with Space Applications," Prentice-Hall, 1964.
- [8] T. Hara, M. Fukui and H. Yamamoto, "Fast and stable Acquisition by Utilizing Multi-Component Code under Very Low C/N Conditions: Application to Acquisition in TDMA Satellite Communications," Electronics and Communications in Japan, Part 1, Vol. 88, No. 5, 2005.

Takao HARA Takao Hara was graduated from the faculty of engineering of Osaka University in Japan in 1968. He received his Ph.D degree in communications engineering from Nara Institute of Science and Technology (NAIST) in 2003. He had been working for Fujitsu Limited for about 35 years before joining the Graduate School of Information Science, NAIST. He worked in Fujitsu America Inc., Washington DC, from 1980 to 1984 for the R&D of TDMA satellite communications in US. He is now an associate professor of NAIST and teaching and studying mobile, radio and satellite communications. He is a member of IEICE and AIAA.

Minoru OKADA Minoru Okada joined Graduate School of Information Science, Nara Institute of Science and Technology in 2000, and is now a professor. He received his B.E. degree in communications engineering from the University of Electro-Communications in 1990 and M.E and Ph.D. degrees both in communications engineering from Osaka University in 1992 and 1998 respectively. From 1999 to 2000, he was with the University of Southampton, U.K. as a Visiting Research Fellow. Dr. Okada's research is in the area of wireless and satellite communications. He is a member of the IEEE, ITEJ, IEICE and IPSJ. He received the Young Engineer Award from IEICE in 1999.

Mayumi OSATO Mayumi Osato received her B.S degree from Nara Women's University and M.E Degrees from the Graduate School of Information Science, Nara Institute of Science and Technology (NAIST) in 2005 and 2007 respectively. She has been engaged in the study and research of mobile and satellite communications. She received best paper award from International Conference on Wireless and Mobile Communications 2007(ICWMC07) on March 2007.

Hiroyuki KOBASHI Hiroyuki Kobashi received his B.E degree from the faculty of engineering of Ehime University and M.E degree from the Graduate School of Information Science, Nara Institute of Science and Technology (NAIST) in 2005 and 2007 respectively. He has been studying and researching satellite communications in the school. He joined JSAT Corporation in April 2007.

Roberto Yusi OMAKI Roberto Yusi Omaki received his B.E., M.E. and Ph.D. degrees in Information Systems Engineering from Osaka University, Osaka, Japan, in 1996, 1998, and 2003, respectively. He joined Synthesis Corporation in 2001 as senior engineer, and was with the Communication Laboratory, Nara Institute of Science and Technology, as a joint researcher in 2006. His research interests include VLSI design, wireless systems and digital signal processing.